ADVANCED ELECTRONIC MATERIALS
www.advelectronicmat.de

Transparent Nanoscale Polyimide Gate Dielectric for Highly Flexible Electronics

*Saungeun Park, Hsiao-Yu Chang, Somayyeh Rahimi, Alvin L. Lee, Li Tao, and Deji Akinwande**

Transparent and solution-processable nanoscale polyimide (NPI) films less than 100 nm thick and their applications as flexible gate dielectrics for 2D-materials-based transistor devices are reported. Stable electrical performances of NPI dielectric under high tensile strains up to 10% are demonstrated by in situ bending experiments. A welcome benefit of the NPI nanoscale thickness is that the optical transparency is improved over 84% across the visible spectrum compared to conventional thick polyimide, indicating suitability for transparent electronics, such as displays and sensors. Prototypical 2D active materials, molybdenum disulfide (MoS_2), and graphene using NPI gate dielectric show outstanding thin-film transistors (TFTs) properties comparable to performances of similar devices using atomic layer deposition (ALD) gate dielectrics. For instance, MoS_2 FETs with NPI dielectric affords maximum field-effect mobility of 30 $cm^2 V^{-1} s^{-1}$ and ON/OFF current ratio >10^7. Graphene FETs (GFETs), fabricated with NPI dielectric, also show DC and radio frequency (RF) performances comparable to similar devices with high-κ dielectrics, such as maximum carrier mobility of ≈5170 $cm^2 V^{-1} s^{-1}$. An extrinsic cutoff frequency ≈6.5 GHz is achieved, which reveals that NPI is also a suitable dielectric for flexible RF TFTs for wireless communication systems.

1. Introduction

Flexible electronics based on mechanically strong compliant materials, such as 2D semiconducting films, has attracted research attention for a wide variety of device applications, such as foldable, bendable, and stretchable communication systems, sensors, and displays.[1–9] In order to fulfill the full potential of 2D semiconductors for flexible thin-film transistors (TFTs), high strain durable, electrically stable, and smooth gate dielectric films are required.[1,3,5,7] Despite the importance of mechanical flexibility of gate dielectric, there have been rather limited studies examining practical flexible gate dielectric systems. Thus far, metal oxide dielectric films, such as Al_2O_3 and HfO_2, which can afford high dielectric constants and are readily deposited by atomic layer deposition (ALD), have been widely utilized to improve transistor electrostatic gate control while providing conformal coverage.[3,6,8,10,11] However, commonly used high-κ and inorganic dielectrics are rigid with low mechanical flexibility limited to around 2% tensile strain with subsequent mechanical cracking which can lead to current leakage path as the failure mechanism at high strains.[6,12,13] The work by Liu et al. proposed vapor phase self-assembled nanodielectric (v-SAND) as a gate dielectric due to its outstanding electrical, optical properties, and compatibility to most plastic substrates.[14] However, performances of organic TFTs using v-SAND degrade during bending because of gate leakage current. On the other hand, several polymeric dielectrics have shown significantly outstanding mechanical flexibility, but operation voltage is usually quite large due to the relatively thick films needed to ensure low gate leakage current.[15–18] Polyimide (PI), among many polymeric dielectrics, has been widely studied as a gate insulator for flexible organic electronics due to its high chemical stability and good insulation properties.[15,16,19] However, it also requires the large operating voltage due to its thickness (typically approaching micrometer thickness). As such, research is warranted on realizing nanoscale (≤100 nm thick) insulating advanced materials that can be used as gate dielectrics for highly flexible TFTs and systems that can substantially exceed the 2% strain limitation of metal oxide films.

In this communication, we report the transparent and solution-processable nanoscale polyimide (NPI) films less than 100 nm thick and its applications as flexible gate dielectrics for 2D materials based transistor devices. Stable electrical performances of NPI dielectric under high tensile strains up to 10% are demonstrated by in situ bending experiment. A welcome benefit of the NPI nanoscale thickness is that the optical transparency is improved over 84% across the visible spectrum compared to conventional thick polyimide, indicating suitability for transparent electronics, such as display and sensor. Prototypical 2D active materials, molybdenum disulfide (MoS_2), and graphene using NPI gate dielectric show outstanding TFT properties comparable to performances of similar devices using ALD gate dielectrics. For instance, MoS_2 field-effect transistors (FETs) with NPI dielectric show both maximum field-effect mobility of 30 $cm^2 V^{-1} s^{-1}$ and ON/OFF current ratio >10^7. Graphene FETs (GFETs),

S. Park, Dr. H.-Y. Chang, Dr. S. Rahimi, Dr. A. L. Lee, Dr. L. Tao, Prof. D. Akinwande
Microelectronics Research Center
The University of Texas at Austin
TX 78758, USA
E-mail: deji@ece.utexas.edu

DOI: 10.1002/aelm.201700043

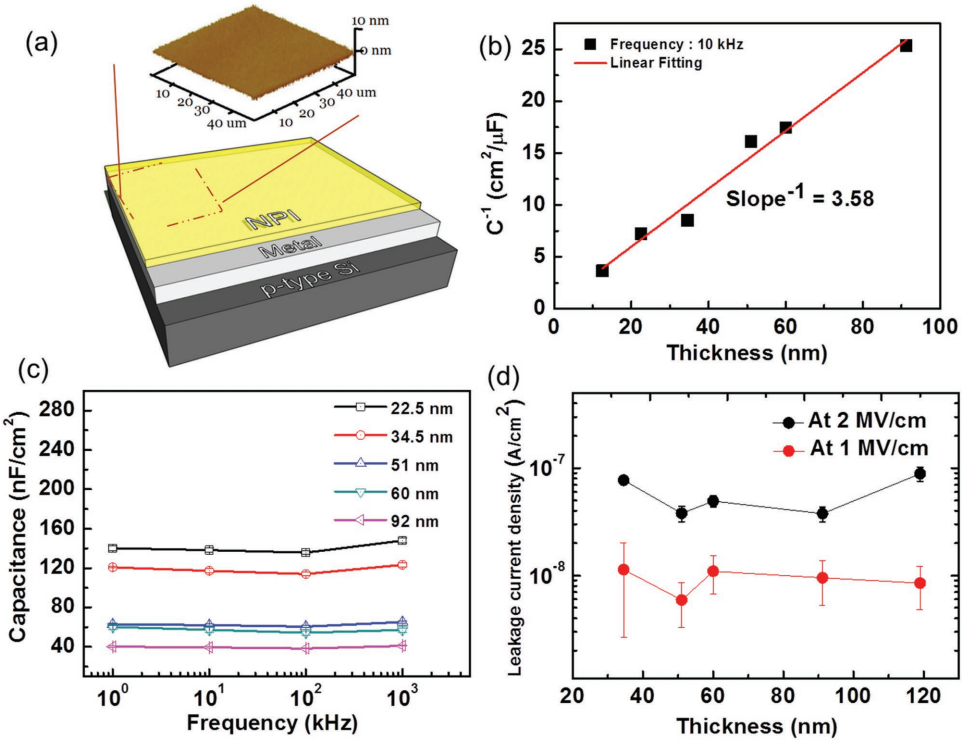

Figure 1. Physical and electrical characterization of nanoscale polyimide thin films. a) NPI surface roughness after curing process on the nickel metal. RMS roughness is less than 0.5 nm for 50 μm × 50 μm area. b) Inverse capacitance as a function of thickness with extracted dielectric constant (≈3.58 ± 0.24) of NPI. c) Capacitance as a function of frequency and thickness. All capacitance values are fairly constant in the wide range of frequency (1 kHz to 1 MHz). d) Leakage current density as a function of thickness at 1 and 2 MV cm^{-1}. Low leakage current density of several film thicknesses at high fields implies the negligible degradation of nanoscale polyimide dielectric after it is properly diluted by NMP.

fabricated with NPI dielectric, also show direct current (DC) and radio frequency (RF) performances comparable to similar devices with high-κ dielectrics, such as maximum carrier mobility of ≈5170 cm^2 V^{-1} s^{-1}.[3,4] An extrinsic cutoff frequency ≈6.5 GHz is achieved, which reveals that NPI is also a suitable dielectric for flexible RF TFTs for wireless communication systems unlike similarly highly flexible ion-gel dielectrics that are limited to kHz frequencies or below.[20]

2. Results and Discussion

Solution processable NPI was obtained through the chemical dilution of liquid polyimide (LPI) precursor (from HD MicroSystems) with *N*-methyl-2-pyrrolidone (NMP) (from Sigma-Aldrich).[16,19] The thickness of NPI can be controlled by the spin-coating speed as well as by controlling the viscosities obtained by different volume ratio mixing of LPI and NMP.[19] A curing process at 250 °C under nitrogen (N_2) atmosphere for 2 h was developed to polymerize the solution-based precursor as well as to drive out the remaining solvent. The temperature profile of the curing process is shown in Figure S1 (Supporting Information). **Figure 1**a shows the surface topography of NPI on the Ni coated highly doped Si substrate after the curing process, and the corresponding root mean square (RMS) roughness is about 0.5 nm over 50 μm × 50 μm area. It should be noted that the NPI dielectric flattens the rough surface of Ni. The RMS roughness of Ni surface was 0.75 nm before NPI dielectric formation. The dielectric constant, κ, is extracted from metal-insulator-metal (MIM) test structures fabricated from metal/NPI/highly doped Si and is determined to be 3.58 ± 0.2 as shown in Figure 1b. Note that the y-intercept of Figure 1b is the interface capacitance which might be due to the native oxide on Si as well as interface traps.[21] Figure 1c represents capacitances (up to 140 Nf cm^{-2}) for different NPI dielectric thicknesses. Figure 1d shows the leakage current densities at the electric field of 1 and 2 MV cm^{-1} with varying thickness. The relatively flat profile with thickness indicates the negligible degradation of electrical characteristics of nanoscale polyimide and outstanding leakage current density compared with other flexible dielectrics (**Table 1**).[6,14,22–25]

In situ bending measurement was conducted using MIM test structures on Kapton substrate in order to systematically study the electrical performance of NPI dielectric under bending strains as illustrated in **Figure 2**a. NPI solution was spin coated on Pd/Kapton followed by curing at 250 °C for 2 h under N_2. Metal contacts (1nm Ti/100 nm Cu) were deposited as a top electrode to complete the device fabrication. The sample with 60 nm NPI was loaded on the in situ bending fixture as shown in Figure S3a (Supporting Information). Optical images of flexible MIM devices under strain up to 10% are shown in Figure S3b–d (Supporting Information). Note that we applied global substrate strain and we will use the term "strain" instead of global substrate strain in following manuscript. MIM devices atop surface, which can be seen by optical microscope, were

Table 1. A comparison of several candidate thin-film gate dielectrics for flexible electronics. NR: Not reported.

	Thickness [nm]	RMS roughness [nm]	Dielectric constant	Dielectric loss	Leakage current density [A cm^{-2}]	Transparency [%]	Strain/bending radius [% mm^{-1}]
Al_2O_3[6]	25	<1	7	NR	NR	NR	2/2.5
Solution-grown amorphous alumina (Al_2Ox)[22]	93	0.78	9.5	NR	NR	>76	NR/10
Mylar[23]	2500	0.7	3.25 @ 1 kHz 3@ 1 MHz	0.005 @ 1 kHz 0.005 @ 1 MHz	NR	NR	1/0.2
Inorganic/organic hybrid dielectric (v-SAND)[14]	20	0.84	4.5 @ 1 kHz 2.25 @ 1 MHz	NR	10^{-6} @1 MV cm^{-1}	≈70	0.56/20
Graphene interlayer[24]	1740	NR	52 @ 1 kHz 10 @1 MHz	0.05 @ 1 kHz >1 @ 1 MHz	10^{-3} @1 MV cm^{-1}	>88	0.83/7.5
Parylene[25]	18	0.76	3.06	NR	10^{-9} @1 MV cm^{-1}	NR	NR/0.8
This work	60	<1	3.58 @ 10 kHz	0.03 @ 1 MHz	10^{-8} 1 MV cm^{-1}	>84	10/0.75

characterized using a semiconductor device parameter analyzer (Agilent B1500A) for current–voltage (I–V) and capacitance-voltage (C–V) characteristics. Figure 2b details the leakage current density as a function of electric fields under flat and 7% tensile strain conditions. Notably, the leakage current density at 7% strain is comparable with that of previously reported flexible dielectrics, such as high-κ dielectric and v-SAND dielectric, without strain.[14,23,26,27] Note that the leakage current density of flexible MIM devices is an order higher than the leakage current of Si-based MIM structure (Figure 1d). We attribute this to the locally enhanced electrical field induced by rough surface of polyimide substrate. Figure 2c,d is the C–V characteristics of NPI at 10 kHz and 5 MHz, where the maximum measurement frequency is limited by the measurement setup. The capacitance variation under up to 10% strain is very small as shown in Figure 2c. In addition, dielectric loss less than 0.04 is measured at strain up to 10% (Figure 2d), suggesting that dielectric relaxation is negligible. Table 1 shows a comparison of some dielectric

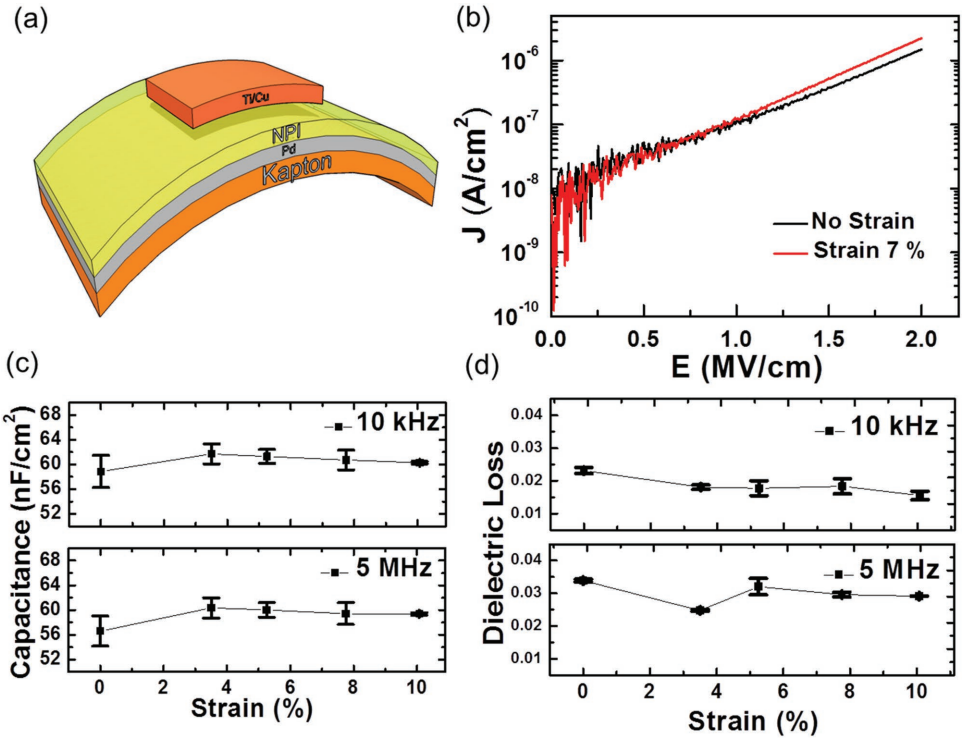

Figure 2. Mechanical performance of nanoscale polyimide dielectric. a) Device schematic representation for the in situ evaluation for electrical stability under mechanical bending. b) Leakage current density as a function of the electric field under flat and 7% tensile strain for 60 nm NPI. The leakage current density of flexible MIM devices is an order higher than the leakage current of Si-based MIM structure (Figure 1d). c,d) Capacitance and dielectric loss as a function of strain up to 10% for 60 nm NPI, respectively. The consistent performance under large bending conditions affords a realistic prospect for advanced (high strain) flexible electronics.

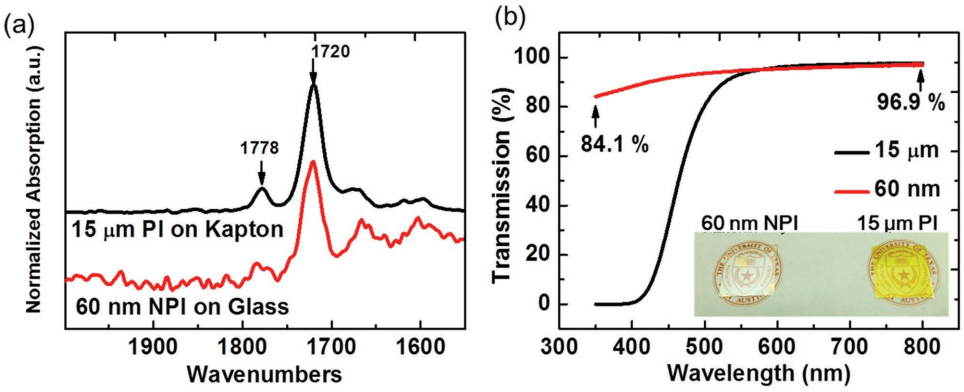

Figure 3. Optical studies of nanoscale polyimide. a) Carbonyl region of the FTIR spectrum of 60 nm NPI on glass and 15 μm thick spin-coated and cured PI on thick Kapton film. Both showed the same characteristic vibration bands near 1778 and 1720 cm^{-1}. b) Optical transparency for PI with thickness of 60 nm and 15 μm on glass substrates. The transparency has improved to more than 84% for NPI for the entire visible spectrum.

properties for various flexible dielectrics that have been reported. Note that this work is the first practical study for in situ electromechanical measurement with up to 10% strain, but other studies on flexible dielectric were done with the ex situ measurement with relatively low strain (measurements were mostly done on flat sample after applying low strain). The stable electrical performances at large bending conditions demonstrate that NPI is a promising flexible dielectric compared to existing alternatives.

Figure 3a shows the carbonyl region of the Fourier-transform infrared spectroscopy (FTIR) spectrum of polyimide.[28] Similar to the 15 μm thick PI on the Kapton film, 60 nm thick NPI on glass had the same characteristic vibration bands near 1778 and 1720 cm^{-1},which are in carbonyl stretching region of the infrared spectra (1600–1800 cm^{-1}). The result is consistent with our expectation since the diluting process is not expected to change the chemical composition of polyimide. The optical transparency of 60 nm NPI is shown in Figure 3b, revealing improved transparency over 84% across the visible spectrum, but the 15 μm thick polyimide is completely opaque at wavelengths below 400 nm due to light absorption in thick PI dielectric. Dependence of optical transmission on the wavelength and the NPI dielectric thickness with different wavelengths is shown in Figure S5a,b (Supporting Information), which reveals that the transmittance of NPI dielectric increases with decreasing NPI thickness according to the Beer–Lambert law (Equation 1)

$$T = e^{-\alpha d} \tag{1}$$

where T is the transmittance; α is the absorption coefficient; and d is the film thickness (path length). The exponential dependence of transmittance on the NPI thickness for low wavelength range (300–450 nm) is shown in Figure S5c–e (Supporting Information) and extracted absorption coefficients for the wavelength region are 2500 ± 320 (for 400 nm wavelength), 25,700 ± 4700 (for 350 nm wavelength), and 10,8000 ± 14,700 (for 300 nm wavelength). The outstanding optical transparency indicates that the NPI film is a suitable candidate for the dielectric for TFTs which requires transparency, encapsulation for solar cells, and orientation films in liquid crystal display devices.

For benchmarking the performance of NPI gate dielectrics, TFTs based on MoS_2 and graphene were fabricated. MoS_2 was prepared by mechanical exfoliation of commercial crystals (from SPI supplies) on highly doped Si substrate which is used as the back gate, and 60 nm thick NPI was spin coated and cured. With this gate stack, the exfoliated MoS_2 flakes with different thicknesses can yield good contrast under optical microscope. Flakes with thickness between 5 and 20 nm were selected and confirmed by atomic force microscopy. Source/drain contacts were defined by electron beam lithography (EBL) and lift-off process of 50 nm Au. A schematic representation of the back-gated MoS_2 device is shown in **Figure 4**a. Devices were patterned with a fixed channel length (1 μm) and had varying channel widths (0.5–3 μm) that are naturally defined by the width of the exfoliated flakes.

Electrical characteristics of the MoS_2 FETs were then evaluated under ambient conditions. Representative transfer (I_D–V_G) characteristics are shown in Figure 4b. An ON/OFF current ratio of $>10^7$ and a subthreshold swing of ≈450 mV dec^{-1} were observed. Linear transport at low fields and current saturation characteristics at high fields can be seen in the output characteristics (Figure 4c). The field-effect mobility is in the range of 8–30 cm^2 V^{-1} s^{-1} for a variety of devices with the same channel length.[29] Importantly, the exfoliated MoS_2 flakes with NPI gate dielectrics show comparable device performance to the back-gated devices fabricated with SiO_2 or high-κ dielectric with the same device structure and fabrication process.[6] As shown in Figure 4d, from the statistics of the mobility extracted from devices with different dielectrics, including SiO_2, high-κ dielectric (Al_2O_3), and NPI (this study), NPI shows comparable mobility to conventional dielectrics in Si fabrication process. This comparative study suggests that NPI is a promising candidate to replace the conventional rigid inorganic dielectrics for highly flexible electronics.

The fabrication of graphene FETs starts from 300 °C curing process of LPI on PI substrate (≈127 μm thick) in order to achieve the RMS roughness less than 1 nm as described in prior works.[3,5] The first EBL patterned a gate array that has embedded gate with six fingers to enhance the current drive; metal contacts (2 nm Ti/38 nm Pd) was deposited for embedded gate electrodes. NPI was spin coated and cured at 250 °C for 2 h, which formed 60 nm of flexible gate dielectric. Gate pad area was opened by the second EBL and CF_4/Ar plasma etching. Monolayer graphene grown on copper foil by chemical vapor deposition was then transferred on the patterned device via poly(methyl methacrylate)

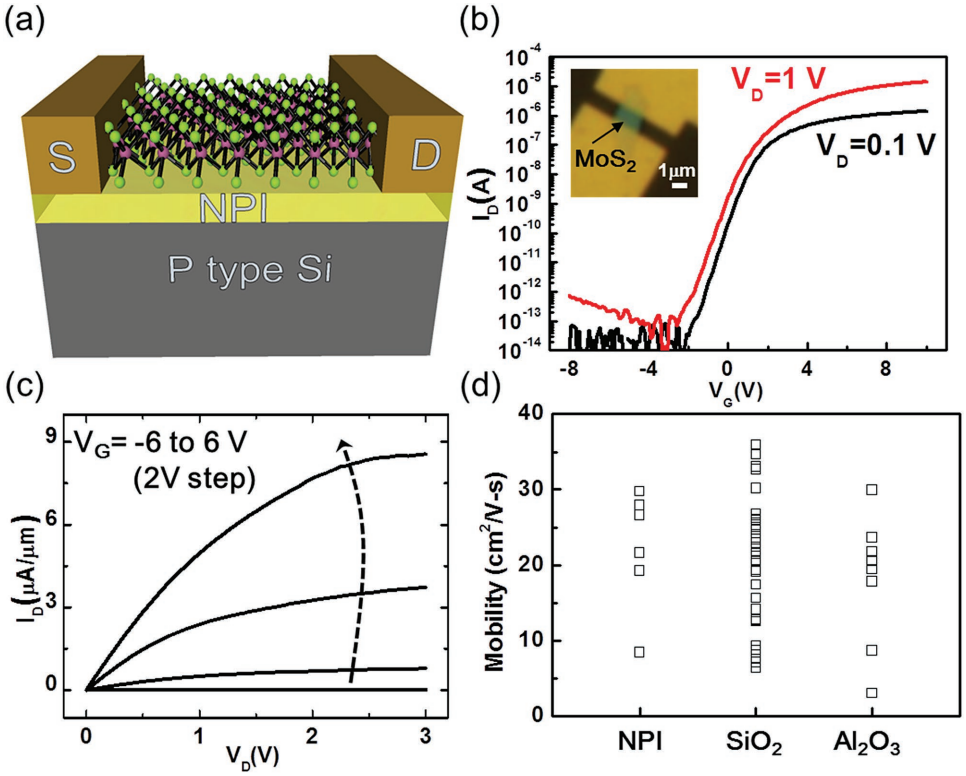

Figure 4. 2D semiconductor (MoS_2) TFT with nanoscale polyimide gate dielectric. a) Schematic depiction of the bottom-gate device. Note that multilayer MoS_2 flakes were used in this study. b) Transfer characteristics of MoS_2 FETs with 60 nm thick NPI dielectric. ON/OFF ratio is larger than 10^7. MoS_2, which is indicated in the insert, is ≈12 nm thick with channel dimensions corresponding to $L = 1$ μm and $W = 1.6$ μm. c) Output characteristics show linear transport at low fields and current saturation at high fields. d) Comparison of the field effect mobility from several samples using NPI, SiO_2, and Al_2O_3 as gate dielectrics. NPI shows comparable mobility to conventional dielectrics in Si fabrication process.

assisted wet transfer process using ammonia persulfate to etch copper film.[30] The third EBL and O_2 plasma were employed to define the active graphene channel. 250 nm and 60 μm of channel length and width were patterned by EBL, respectively. Afterward, the source/drain contacts (1 nm Ti/50 nm Au) were defined and deposited using e-beam evaporation technique.

The transfer characteristic of a completed GFET (**Figure 5**a) on the flexible Kapton substrate is shown in Figure 5b. The hole and electron mobilities, extracted using a widely accepted diffusive transport model,[31] are 1880 and 5170 cm^2 V^{-1} s^{-1}, respectively, with corresponding contact resistances of 1380 and 1830 Ω μm for holes and electrons. Residual carrier concentrations are about ≈4×10^{11} cm^{-2}, which is in good agreement with a previous study using Al_2O_3 dielectrics.[3] The asymmetric transfer characteristic is attributed to high work-function metal at source and drain, which induces additional junction resistance in the electron branch. Electromechanical performances of flexible graphene FETs with NPI dielectric are shown in Figure S6 (Supporting Information). Device performances degrade with increasing strain due to Ohmic loss at S/D contacts. Importantly, leakage current (I_G) is independent on applied strain up to 10%. Microwave performance was characterized from 0.5 to 30 GHz using Agilent two-port network analyzer (VNA-E8361C), and the extrinsic cutoff frequency ($f_{T,ext}$) of this device is as high as 6.5 GHz at a drain voltage of 0.5 V as shown in Figure 5d. The $f_{T,ext}$ is higher than the reported value that was extracted from the similar device structure with the embedded gate and high-k gate dielectrics. The improvement in $f_{T,ext}$ can be attributed to about 3.5 times shorter channel length, significantly reduced contact resistance, and parasitic capacitances between gate and drain (or source).

3. Conclusion

In conclusion, the first comprehensive studies of transparent and solution-based NPI thin films for highly flexible gate dielectrics are demonstrated by in situ optoelectromechanical measurements and utilize for 2D material-based transistors. Stable electrical characteristics of NPI are demonstrated up to 10% tensile strain, and transparency higher than 84% over the visible spectrum is achieved. Molybdenum disulfide FETs with NPI dielectric show outstanding DC performance, including 30 cm^2 V^{-1} s^{-1} for the highest field-effect mobility and >10^7 ON/OFF current ratio, which are comparable to performances from conventional dielectrics in Si fabrication process. Graphene FETs using NPI dielectric afford outstanding DC and RF characteristics including maximum mobility of 5170 cm^2 V^{-1} s^{-1} and extrinsic cutoff frequency of 6.5 GHz.

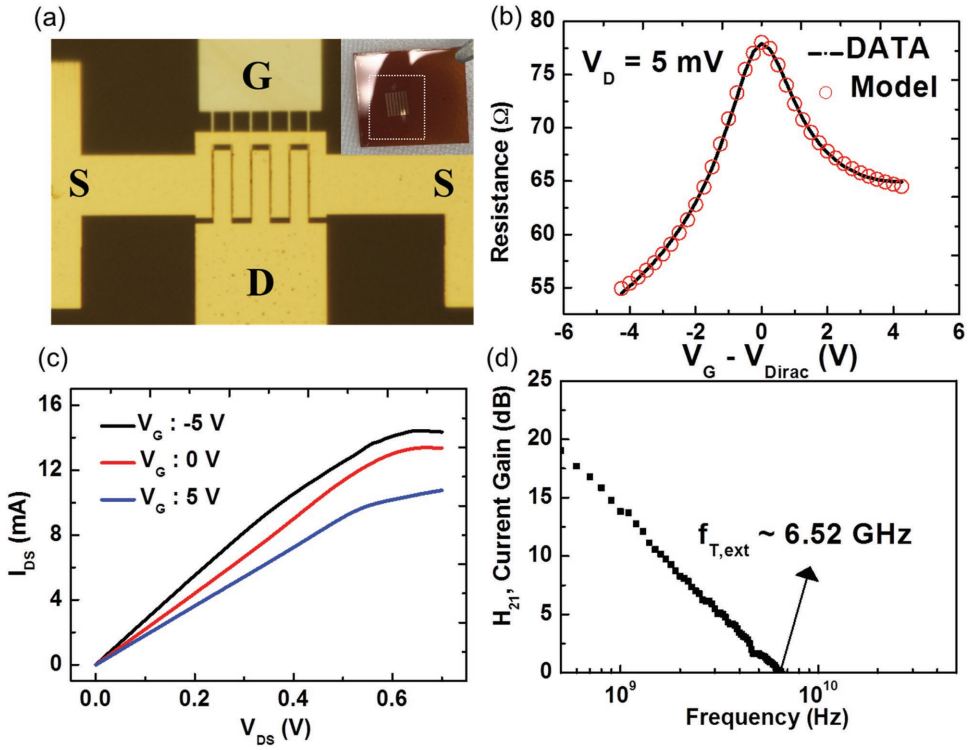

Figure 5. Flexible graphene transistor using nanoscale polyimide gate dielectric. a) An optical image of the embedded-gate graphene TFTs. Channel width and length are 60 µm and 250 nm, respectively. b) Transfer characteristics of graphene TFTs with 60 nm thick NPI gate dielectric. Extracted mobilities for hole and electron are 1880 and 5170 $cm^2 V^{-1} s^{-1}$, respectively. c) Output characteristics with various gate voltages from –5 to 5 V with gate voltage step of 5 V, which show weak current saturation at high fields. d) Current gain as a function of frequency. The extrinsic cutoff frequency from measured S-parameters is about 6.5 GHz.

Supporting Information

Supporting Information is available from the Wiley Online Library or from the author.

Acknowledgements

This work was supported in part by the Office of Naval Research and the NSF-NASCENT Engineering Research Center (Cooperative Agreement No. EEC-1160494). Fabrication was conducted at Microelectronics Research Center, an NSF supported NNCI Center at the University of Texas at Austin. The authors also acknowledge assistance from Avinash Nayak for UV–vis measurements.

Conflict of Interest

The authors declare no conflict of interest.

Keywords

2D materials, analog device, flexible gate dielectric, graphene, mobility, molybdenum disulfide, RF

Received: February 2, 2017
Revised: November 15, 2017
Published online:

[1] D. Akinwande, N. Petrone, J. Hone, *Nat. Commun.* **2014**, *5*, 12.
[2] S. Rumyantsev, G. Liu, M. S. Shur, R. A. Potyrailo, A. A. Balandin, *Nano Lett.* **2012**, *12*, 2294.
[3] J. Lee, T.-J. Ha, H. Li, K. N. Parrish, M. Holt, A. Dodabalapur, R. S. Ruoff, D. Akinwande, *ACS Nano* **2013**, *7*, 7744.
[4] J. Lee, K. N. Parrish, S. F. Chowdhury, T. J. Ha, Y. F. Hao, L. Tao, A. Dodabalapur, R. S. Ruoff, D. Akinwande, *IEEE, 2012 IEEE International Electron Devices Meeting (Iedm)*, San Francisco, CA, USA **2012**, 4.
[5] J. Lee, L. Tao, K. N. Parrish, Y. F. Hao, R. S. Ruoff, D. Akinwande, *IEEE, 2012 12th IEEE Conference on Nanotechnology (IEEE-Nano)*, **2012**, 3.
[6] H. Y. Chang, S. X. Yang, J. H. Lee, L. Tao, W. S. Hwang, D. Jena, N. S. Lu, D. Akinwande, *ACS Nano* **2013**, *7*, 5446.
[7] G. H. Lee, Y. J. Yu, X. Cui, N. Petrone, C. H. Lee, M. S. Choi, D. Y. Lee, C. Lee, W. J. Yoo, K. Watanabe, T. Taniguchi, C. Nuckolls, P. Kim, J. Hone, *ACS Nano* **2013**, *7*, 7931.
[8] W. N. Zhu, M. N. Yogeesh, S. X. Yang, S. H. Aldave, J. S. Kim, S. Sonde, L. Tao, N. S. Lu, D. Akinwande, *Nano Lett.* **2015**, *15*, 1883.
[9] S. Das, R. Gulotty, A. V. Sumant, A. Roelofs, *Nano Lett.* **2014**, *14*, 2861.
[10] M. E. Ramon, K. N. Parrish, S. F. Chowdhury, C. W. Magnuson, H. C. P. Movva, R. S. Ruoff, S. K. Banerjee, D. Akinwande, *IEEE Trans. Nanotechnol.* **2012**, *11*, 877.
[11] A. Javey, J. Guo, D. B. Farmer, Q. Wang, D. W. Wang, R. G. Gordon, M. Lundstrom, H. J. Dai, *Nano Lett.* **2004**, *4*, 447.
[12] Y. G. Seol, H. Y. Noh, S. S. Lee, J. H. Ahn, N. E. Lee, *Appl. Phys. Lett.* **2008**, *93*, 3.
[13] S. H. Jen, J. A. Bertrand, S. M. George, *J. Appl. Phys.* **2011**, *109*, 084305.

[14] J. Liu, D. B. Buchholz, R. P. H. Chang, A. Facchetti, T. J. Marks, *Adv. Mater.* **2010**, *22*, 2333.
[15] H. Ohuchi, Y. Takayanagi, H. Yano, Z. F. Duan, T. Okukawa, Y. Yanagi, A. Yoshida, Y. Nishioka, *J. Photopolym. Sci. Technol.* **2012**, *25*, 381.
[16] Y. Noguchi, T. Sekitani, T. Someya, *Appl. Phys. Lett.* **2006**, *89*, 3.
[17] A. Loi, I. Manunza, A. Bonfiglio, *Appl. Phys. Lett.* **2005**, *86*, 103512.
[18] H. T. Yi, M. M. Payne, J. E. Anthony, V. Podzorov, *Nat. Commun.* **2012**, *3,* 7.
[19] Y. Kato, S. Iba, R. Teramoto, T. Sekitani, T. Someya, H. Kawaguchi, T. Sakurai, *Appl. Phys. Lett.* **2004**, *84*, 3789.
[20] J. Pu, Y. Yomogida, K. K. Liu, L. J. Li, Y. Iwasa, T. Takenobu, *Nano Lett.* **2012**, *12*, 4013.
[21] B. Fallahazad, K. Lee, G. Lian, S. Kim, C. M. Corbet, D. A. Ferrer, L. Colombo, E. Tutuc, *Appl. Phys. Lett.* **2012**, *100*, 4.
[22] X. Yu, N. Zhou, P. Guo, F. Shi, D. B. Buchholz, Q. Ma, J. Yu, V. P. Dravid, R. P. H. Chang, M. Bedzyk, T. J. Marks, A. Facchetti, *Adv. Mater.* **2015**, *27*, 2390.
[23] H. T. Yi, Y. Chen, K. Czelen, V. Podzorov, *Adv. Mater.* **2011**, *23*, 5807.
[24] J. Y. Kim, J. Lee, W. H. Lee, I. N. Kholmanov, J. W. Suk, T. Kim, Y. F. Hao, H. Chou, D. Akinwande, R. S. Ruoff, *ACS Nano* **2014**, *8*, 269.
[25] M. Kondo, T. Uemura, T. Matsumoto, T. Araki, S. Yoshimoto, T. Sekitani, *Appl. Phys. Lett.* **2016**, *9*, 061602.
[26] M. D. Groner, J. W. Elam, F. H. Fabreguette, S. M. George, *Thin Solid Films* **2002**, *413*, 186.
[27] H. C. Lin, P. D. Ye, *Appl. Phys. Lett.* **2005**, *87*, 182904.
[28] R. W. Snyder, B. Thomson, B. Bartges, D. Czerniawski, P. C. Painter, *Macromolecules* **1989**, *22*, 4166.
[29] H. Y. Chang, W. N. Zhu, D. Akinwande, *Appl. Phys. Lett.* **2014**, *104*, 113504.
[30] S. Rahimi, L. Tao, S. F. Chowdhury, S. Park, A. Jouvray, S. Buttress, N. Rupesinghe, K. Teo, D. Akinwande, *ACS Nano* **2014**, *8*, 10471.
[31] S. Kim, J. Nah, I. Jo, D. Shahrjerdi, L. Colombo, Z. Yao, E. Tutuc, S. K. Banerjee, *Appl. Phys. Lett.* **2009**, *94*, 3.

